The application of a vacuum-ultraviolet Fourier transform spectrometer and synchrotron-radiation source to measurements of bands of NO. VII. The final report

K. Yoshino[a)]
Harvard-Smithsonian Center for Astrophysics, Cambridge, Massachusetts 02138

A. P. Thorne and J. E. Murray
Blackett Laboratory, Imperial College, London, SW7-2BZ, United Kingdom

A. S.-C. Cheung and A. L. Wong
Department of Chemistry, The University of Hong Kong, Hong Kong

T. Imajo
Japan Women's University, Tokyo 112-8681, Japan

(Received 28 September 2005; accepted 25 October 2005; published online 7 February 2006)

Photoabsorption measurements of NO bands have been made by vacuum-ultraviolet Fourier transform spectrometry with a resolution of 0.12 cm^{-1} in the wavelength region of 166.2–196.2 nm. Accurate line positions are obtained for the $\delta(v,0)$ bands with $v=2$, 3, the $\epsilon(v,0)$ bands with $v=2$, 3, and the $\beta(v,0)$ bands with $v=10,12,14$. Absolute term values are found for the corresponding upper levels $C(2,3)$, $D(2,3)$, and $B(10,12,14)$. Accurate rotational line integrated cross sections have also been obtained for the lines in these bands. Integrated cross sections reported in our earlier papers [J. Chem. Phys. **109**, 1751 (1998); **112**, 2251 (2000); **115**, 3719 (2001); **116**, 155 (2002); **117**, 10621 (2002); **119**, 8373 (2003)] have been revised, and the results reported here comprise the $\delta(v,0)$ bands with $v=0-3$, the $\epsilon(v,0)$ bands with $v=0-3$, the $\beta(v,0)$ bands with $v=6,7,9-12,14$, and the $\gamma(3,0)$ band. For each band, the band oscillator strength is obtained from the sum of the line strengths of all rotational lines, and these are compared with other published values. © *2006 American Institute of Physics*. [DOI: 10.1063/1.2138029]

I. INTRODUCTION

In a series of papers over the last few years we have reported measurements of accurate line positions and intensities of various bands: the γ band [$A\ ^2\Sigma^+$-$X\ ^2\Pi_r$], the β band [$B\ ^2\Pi_r$-$X\ ^2\Pi_r$], the δ band [$C\ ^2\Pi_r$-$X\ ^2\Pi_r$], and the ϵ band [$D\ ^2\Sigma^+$-$X\ ^2\Pi_r$] of NO between 180 and 198 nm, measured in absorption with a vacuum-ultraviolet Fourier transform spectrometer.[1–6] These measurements are needed for reliable modeling of the photodestruction of NO by solar radiation in the middle atmosphere. The absorption lines are narrow, and the necessity for high-resolution measurements to yield true cross sections has been discussed in our earlier papers.[1–3] To achieve the necessary resolution we combined vacuum-ultraviolet (vuv) Fourier transform spectrometry (FTS) with synchrotron radiation by taking the Imperial College (IC) vuv FT spectrometer to the synchrotron-radiation source at Photon Factory (PF), KEK, Japan, where a suitable zero dispersion two-grating predisperser is available on beamline 12-B. [The predisperser is necessary to limit the bandwidth to a few nanometers in order to achieve acceptable signal-to-noise (S/N) ratios.] We have used this combination of facilities to make ultrahigh-resolution cross-section measurements of NO in the wavelength region of 160–195 nm.

Our six earlier papers[1–6] give line wave numbers, integrated cross sections, and band oscillator strengths for the $\delta(1,0)$, $\epsilon(0,0)$, $\epsilon(1,0)$, $\beta(6,0)$, $\beta(9,0)$, $\beta(11,0)$, and $\gamma(3,0)$ bands together with term values and molecular constants for the corresponding upper levels: $C(1)$, $D(0,1)$, $B(6,9,11)$, and $A(3)$. An additional paper[7] discussed the absolute wavenumber calibration of the FT spectra and made some small corrections (less than 0.1 cm^{-1}) to the line positions and term values of some of the bands. Prior to the work at PF, we also made measurements by FTS of the $\delta(0,0)$ and $\beta(7,0)$ bands, using a hydrogen discharge source as the background continuum;[8] these yielded accurate line positions, together with term values for $C(0)$ and $B(7)$, but larger uncertainties in line intensities owing to low signal-to-noise ratio and uncertain column density measurements.

Herzberg *et al.*[9] have made a rotational analysis of the δ and β bands without publishing the observed line list. They pointed out the interaction of the $C(2)$ and $B(12)$ levels and also the $C(3)$ and $B(15)$ levels, the band origins of which are shifted in opposite directions by about 80 and 200 cm^{-1}, respectively. Higher levels are almost completely mixed. Lagerqvist and Miescher[10] presented the entire line lists of the δ and β bands, and discussed the interaction between the $C\ ^2\Pi$ and $B\ ^2\Pi$ states. They mentioned that the lower J levels of the $C(2)$ level are perturbed by the $B(12)$ level, and the high J levels by the $B(13)$ level. Gallusser and Dressler[11] studied theoretically the homogeneous perturbation of the $^2\Pi$ state of

a)Author to whom correspondence should be addressed. Electronic mail: kyoshino@cfa.harvard.edu

NO, and presented the perturbed and unperturbed band origins, the rotational constants, and the band oscillator strengths for the δ and β bands. Raoult[12] made a more complete study of the perturbation of $^2\Pi$-$^2\Pi$ Rydberg-valance states by using generalized quantum-defect theory. Recently Braun *et al.*[13] observed the $E\,^2\Sigma^+$-$C\,^2\Pi$ bands ($\Delta v=0$) in emission with a high-resolution Fourier transform spectrometer in the infrared region and tabulated the term values of the A, D, E, and C states for $v=0-2$. Their values are compared with those from our previous papers in Ref. 7.

The cross-section measurements of NO bands by Bethke[14] were performed at low resolution, 0.04 nm, in the presence of high-pressure Ar. The addition of the argon buffer gas ensured that the rotational lines were broadened beyond the instrumental resolution, allowing the true cross section to be presented. Guest and Lee[15] used a synchrotron source and resolution of 0.03 nm for the cross-section measurements at very low pressure of NO gas, $2\times10^{-4}-7\times10^{-2}$ Torr. Chan *et al.*[16] used the high-resolution dipole (e,e) technique, which is not sensitive to the instrumental resolution. Luque and Crosley[17] calculated the band oscillator strengths of the A-X and D-X systems. Very recently, Mayor *et al.*[18] calculated the integrated cross section of rotational line of the $\delta(0,0)$ band of NO with the molecular quantum-defect orbital methology, and they compared their results with our previous results.[8]

In this paper we report the results of analysis of all the other bands observed with the synchrotron-FTS combination: $\delta(2,0)$, $\delta(3,0)$, $\beta(10,0)$, $\beta(12,0)$, $\beta(14,0)$, $\epsilon(2,0)$, and $\epsilon(3,0)$, together with new measurements of $\delta(0,0)$ and $\beta(7,0)$. The uncertainty in the absolute wave numbers and term values is 0.03 cm^{-1} after calibration.[7] The band oscillator strengths have been determined from line-by-line measurements because the spectral resolution is comparable with the Doppler widths of the lines.

II. EXPERIMENT

Details of the experimental procedures for recording high-resolution FT spectra of NO between 160 and 198 nm have been described in our earlier publications.[1,2] Only a brief description of the experimental conditions will be given here. The optical path length and the pressure of NO gas depend on the particular band. The column densities of NO in these experiments were 8.32×10^{15} mol cm^{-2} for the $\delta(0,0)$ and $\beta(7,0)$ bands, 9.24×10^{15} mol cm^{-2} for the $\delta(2,0)$ and $\beta(12,0)$ bands, 1.47×10^{16} mol cm^{-2} for the $\epsilon(2,0)$ band, 2.06×10^{16} mol cm^{-2} for the $\delta(3,0)$ band, 3.70×10^{16} mol cm^{-2} for the $\epsilon(3,0)$ band, 2.10×10^{17} mol cm^{-2} for the $\beta(14,0)$ band, and 2.22×10^{17} mol cm^{-2} for the $\beta(10,0)$ band. The signal-to-noise ratios in the continuum background were 34 to 70 depending on the wave numbers.

The transmission spectra were converted to optical depth by taking the logarithms of the intensity and fitting a smooth continuum to the regions between the lines. The absorption lines were fitted to Voigt profiles using the spectral reduction routine GREMLIN.[19] Line parameters such as line position, linewidth, and integrated intensity of individual lines were determined through a nonlinear least-squares iterative procedure. The Voigt profile for the NO lines should be a convolution of a Gaussian due to the Doppler broadening and a Lorentzian arising from predissociation. In this case the Gaussian component of the best-fit Voigt function had a full width at half maximum (FWHM) of 0.175 cm^{-1} which is significantly larger than the value of 0.12 cm^{-1} expected for the Doppler width in our experimental conditions. This anomalous Gaussian width is considered to be due to drifts in alignment causing very small wave-number shifts over the long observation periods.[20]

As discussed in the previous paper[7] on absolute wave-number calibration, the FTS scaling factor can be treated as a constant shift over the limited wave-number range of a single band. A directly measured shift of +0.087 cm^{-1} has been applied to the $\beta(10,0)$ band and a shift of +0.083 cm^{-1} (the mean value of all the directly measured shifts) to all the other bands. The uncertainty in the absolute wave numbers is 0.03 cm^{-1}, while the relative uncertainty is 0.01 cm^{-1} for the strongest lines.

As pointed out by Hudson and Carter,[21] most cross-section measurements for molecular bands with fine rotational structures are severely distorted by the instrumental bandwidths. Plots of optical depth versus column density are never linear unless the spectral features are very much broader than the instrumental widths. All measured cross sections are weighted averages over the instrumental widths, so that the measured peak cross sections of the lines are lower limits to the true values and the wing cross sections are the upper limits. On the other hand, the integrated cross sections are much less sensitive to the instrumental width, and for the lines of small optical depth ("optically thin" lines) they are independent of instrumental width. We discussed these effects in more detail in the Appendix of Stark *et al.*[22] In the present measurements we set the resolution of the FT spectrometer to 0.06 cm^{-1}, about half of the Doppler width, to avoid the effects of the instrumental function, since the ratio of measured to true integrated cross sections for a line of optical depth 1.5 should then be 0.98, within the experimental uncertainty. However, as explained above, the resolution is degraded to around 0.12 cm^{-1} by the alignment drift, and the effect on the integrated cross sections of the stronger lines becomes significant. We calculated the size of the effect for a Gaussian instrumental function of width 0.12 cm^{-1}, equal to the Doppler width. (The FTS sinc instrument function convolved with a rectangular shift function of appropriate width can be closely approximated by a Gaussian.) The ratio of measured to true cross section varies from 0.93 at a measured optical depth of 0.5 to 0.77 at a measured optical depth of 1.5. We have applied an optical path-dependent correction based on this calculation to each observed line.

III. RESULTS AND DISCUSSION

A. Line positions and term values

The $\delta(0,0)$ and $\beta(7,0)$ bands in the wavelength region of 190–192 nm were recorded in our earlier work with the FT spectrometer,[8] but we repeated the measurements of these bands for consistency of the series. We found complete

agreement in line position measurements between the previous[8] and present work, with average differences of 0.001 ± 0.017 cm^{-1}, so we do not repeat the line positions and term values in this paper.

The absolute line wave numbers of the β bands (10,0), (12,0), and (14,0); the δ bands (2,0) and (3,0); and the ϵ bands (2,0) and (3,0) are presented in Table I. The $\beta(10,0)$ band is observed in the wavelength region of 181.5–182.7 nm, in the shoulder of the strong $\delta(1,0)$ band, and the line positions are given in Table Ia. The upper levels of the $C(1)$ and $B(10)$ levels are perturbed around $J=13$, and the lines with $J>13$ are the tails of the $\delta(1,0)$ band. However, the bands appear as two separate bands and are presented in this way. The high column density used in these measurements allowed us to assign ten additional weak lines belonging to the $\delta(1,0)$ band,[2] and these are also presented in Table Ia. The $\delta(2,0)$ and $\beta(12,0)$ bands are observed in the wavelength region of 174.9–177.1 nm. Both bands appear with similar intensity, and their upper levels, $C(2)$ and $B(12)$, perturb each other strongly. The high J of the $C(2)$ level are also perturbed by the $B(13)$ levels.[23] A Λ-type doubling is observed for the $\delta(2,0)$ band, except for the low J lines, but not for the $\beta(12,0)$ band. These results are presented in Tables Ib and Ic for the $\beta(12,0)$ and $\delta(2,0)$ bands, respectively. The $\epsilon(2,0)$ and $\beta(13,0)$ bands are observed in the wavelength regions of 172.3–173.5 and 170.7–172.1 nm, respectively. Heterogeneous perturbation of the $D(2)$ and $B(14)$ levels is expected, but occurs at high J values beyond the limit of our observations. The results are presented in Tables Id and Ib for the $\epsilon(2,0)$ and $\beta(14,0)$ bands, respectively. The $\delta(3,0)$ band is observed in the wavelength region of 168.8–169.6 nm and is presented in Table Ic. The upper level of the $\delta(3,0)$ band is perturbed strongly by the $B(15)$ level (not observed in these measurements).[23] The $\epsilon(3,0)$ band is observed in the wavelength region of 166.3–167.2 nm and is presented in Table Id. We were able to extend the assignment of lines by comparison with Miescher,[24] and the band head areas of the P_{11} and $P_{21}+Q_{11}$ branches are reassigned.

The NO $^2\Pi$ multistate interaction is a well-known perturbation that has been examined in detail.[11,23] The $B\,^2\Pi$-$C\,^2\Pi$ interaction is so strong that it is insufficient to consider only pairwise $B(12)\,^2\Pi$-$C(2)\,^2\Pi$ or $B(15)\,^2\Pi$-C(3) $^2\Pi$ vibrational level interaction. Every rotational level of the B-C complex is significantly mixed. A quantitative analysis of the observations in terms of the five electronic states $B\,^2\Pi$, $C\,^2\Pi$, $K\,^2\Pi$, $L\,^2\Pi$, and $Q\,^2\Pi$ was performed by Gallusser and Dressler.[11] The coupling is treated with a vibronic interaction matrix that includes the bound vibrational levels of these five states. Both components of the spin doublets and three different isotopes are included, and the calculated energies and B values of the perturbed vibronic levels are fitted to the experimental data in the determination of RKR potential curves and off-diagonal electronic energy. The results include predicted oscillator strengths for all the bands as well as detailed rotational structures for complex multistate interactions. In view of the comprehensive work performed by Gallusser and Dressler,[11] we could not undertake any least-squares fitting with the few bands that we observed in this energy region.

The rotational term values of the upper states were obtained by adding the term values of the $v=0$ level of the $X\,^2\Pi$ state to the wave numbers of the observed transition lines. Accurate rotational term values of the $X\,^2\Pi$ state reported by Amiot *et al.*[25] by using high-resolution FT infrared spectroscopy were used, for which the $\Omega=1/2$, $J=0.5$, and e level was taken as the relative zero. The upper-state term values obtained from various branches were averaged only from isolated lines when possible, but the term values are followed by "B" if all branch lines are blended. The results are listed in Table IIa for the $B(10)\,^2\Pi$ and $C(1)\,^2\Pi$ levels; in Table IIb for the $B\,^2\Pi$ levels with $v=12$, 14; in Table IIc for the $C\,^2\Pi$ levels with $v=2$, 3; and in Table IId for the $D\,^2\Sigma$ levels with $v=2$, 3.

Table IIa for the $B(10,0)$ levels also includes the $C(1)$ levels, most of which were published in an earlier paper,[2] because the relevant spectrum was taken at a much higher column density, allowing us to extend the measurements to weak high J lines of the $\delta(1,0)$ band. The term values for $B(10)$ and $C(1)$ are plotted against $J(J+1)$ in Fig. 1. The two curves cross around $J=19.5$, corresponding to $J(J+1)=400$, and the mixing of intensity is discussed in Sec. III B. The $B(12)$ levels (Table IIb) are perturbed strongly by the $C(2)$ level, and so it is not possible to present the molecular constants. Gallusser and Dressler[11] calculated the perturbed rotational constants at $J=0$. Their values are 1.524 and 1.484 cm^{-1} for the F_1 and F_2 levels of the $C(2)$ level, and our observed values are 1.439 and 1.583 cm^{-1}. Their values for the $B(12)$ level are 1.267 and 1.311 cm^{-1} for the F_1 and F_2 levels, and our observed values are 1.230 and 1.377 cm^{-1}. The molecular constants of the $B(14)$ levels are presented in Table IIb, because the heterogeneous interaction with the $D(2)$ level occurs at high J beyond of our observation. The $C(3)$ levels are also strongly perturbed, and the molecular constants are not presented. The heterogeneous perturbation of the $^2\Sigma-{}^2\Pi$ states of NO was discussed by Jungen and Miescher.[26] Fitting for the molecular constants is limited to terms up to $J=15.5$ and 20.5 for the $D(2)$ and $D(3)$ levels, respectively, because the high J levels are shifted by the heterogeneous perturbation of the $B(14)$ and $B(16)$ levels.

The term values reported by Braun *et al.*[13] for the $v=2$ levels can be compared with our $C(2)$ and $D(2)$ levels. The absolute values of Braun *et al.* depend on the UV measurements of the older grating measurements of Engleman and Rouse[27] with an uncertainty of 0.1 cm^{-1}. Our values for the $v=2$ levels are larger than those of Braun *et al.* by 0.08 ± 0.03 cm^{-1} on average, well within the combined uncertainties. We reported in Ref. 7 that the mean difference between our values for the $v=0$, 1 levels and those of Braun *et al.* is only 0.017 cm^{-1}.

B. Integrated cross sections and oscillator strengths

The fitting procedure employed under GREMLIN Ref. 19 also evaluates areas and hence integrated cross sections for the lines fitted. However, these are distorted by the instrumental function, as stated in Sec. II. This effect was not taken into account for our previously published integrated cross sections,[1–6] the band oscillator strengths of which are

TABLE I. Observed wave numbers of the NO bands: $\beta(10,0)$, $\beta(12,0)$, $\beta(14,0)$, $\delta(2,0)$, $\delta(3,0)$, $\epsilon(2,0)$, and $\epsilon(3,0)$ cm^{-1}. Lines followed by B are blended and observed as a single line.

(a) $\beta(10,0)$ band $[B(10)\text{-}X(0)]$

J	R_{11}	Q_{11}	P_{11}	R_{22}	Q_{22}	P_{22}
0.5	55 093.58B	55 090.63				
1.5	55 093.58B	55 088.56	55 085.43B	55 018.69	55 013.46	
2.5	55 092.19	55 085.43B	55 080.06B	55 017.28B	55 010.07	55 004.98b
3.5	55 073.38B		55 089.45	55 014.68B	55 005.31B	54 998.59B
4.5	55 085.43B		55 065.34B	55 010.68	54 999.23	54 989.84
5.5	55 080.06B		55 055.98B	55 005.31B		54 980.17B
6.5	55 073.38B		55 045.29B	54 998.59B		54 969.42
7.5	55 065.34B		55 033.19B	54 990.58		54 957.20
8.5	55 055.98B		55 019.77	54 981.24		54 943.62
9.5	55 045.29B		55 005.31B	54 970.58		54 928.33B
10.5	55 033.19B		54 989.04	54 958.73		54 912.76B
11.5	55 019.77B					54 895.03
12.5	55 005.31B					

Some additional lines of $\delta(1,0)$ band $[(C(1)\text{-}X(0)]$

	R_{11}		P_{11}		R_{22}		R_{21}		P_{21}		R_{11}		R_{21}	
J	*ee*	*ff*	*ee*	*ff*	*ee*	*ff*	*ee*	*ff*	*ee*	*ff*	*ee*	*ff*	*ee*	*ff*
13.5														
14.5	54 975.40													
15.5	54 959.11													
16.5	54 943.06		54 868.47		54 866.72	54 865.87			54 999.66	54 998.59B			54 856.40	54 852.06
17.5	54 928.329B		54 845.46		54 851.75b	54 850.18B			54 986.11	54 984.41			54 862.68B	54 858.72B
18.5	54 916.10	54 916.64	54 822.73		54 840.41B	54 837.69			54 976.43	54 973.48B			54 863.74	54 860.77B
19.5	54 906.78	54 908.51B	54 801.33B		54 835.90B	54 831.30			54 973.48B	54 968.76	54 795.09	54 799.88B		
20.5	54 900.78	54 904.52	54 782.44	54 782.98	54 838.60	54 831.91B	54 842.65B	54 839.93	54 977.94	54 971.46	54 785.60	54 787.35		
21.5	54 900.31	54 906.07	54 766.46	54 768.19	54 846.93B	54 839.17	54 833.14	54 828.43	54 988.01	54 980.17B				
22.5	54 905.48	54 912.76B	54 753.77	54 757.38B	54 858.72	54 849.72B	54 831.00	54 824.32B	55 001.54	54 992.44				
23.5	54 914.40	54 922.94	54 746.38B	54 752.35B	54 872.44B	54 862.68B	54 834.36	54 826.42	55 017.28B	55 007.13				
24.5	54 925.79	54 935.26	54 745.16	54 752.35B	54 887.70	54 876.84	54 841.23	54 832.20	55 034.37	55 023.35				
25.5	54 938.64	54 949.06	54 747.54B	54 755.82B	54 903.88	54 892.12	54 850.18B	54 840.41B	55 052.53	55 040.57				
26.5	54 952.56	54 963.88	54 752.35B	54 762.58B	54 920.79	54 908.51B	54 860.77B	54 849.72B	55 071.46	55 058.66				
27.5	54 967.29	54 979.46	54 758.87	54 768.68B			54 872.44B	54 860.77B						
28.5	54 982.67	54 995.65	54 765.74B	54 776.88										
29.5	54 998.05	55 012.23	54 773.76	54 785.60B										
30.5	55 014.62B	55 028.99												

(b) $\beta(12,0)$ band $[B(12)\text{-}X(0)]$

J	R_{11}	Q_{11}	P_{11}	R_{12}	R_{22}	Q_{22}	P_{22}
0.5	56 742.91	56 739.28					
1.5	56 744.08B	56 737.88	56 734.22		56 656.34	56 649.46	

TABLE I. (*Continued.*)

2.5	56 744.08B	56 735.64	56 729.54	56 623.99B	56 657.45B	56 647.75	56 640.84
3.5	56 743.37	56 732.49	56 723.82B	56 623.14B	56 657.45B	56 645.32	56 635.70
4.5	56 741.60	56 728.37	56 717.42	56 620.11	56 656.86B	56 641.81B	56 629.85
5.5	56 738.82		56 709.93	56 617.40	56 655.18	56 637.94	56 623.14B
6.5	56 734.95		56 701.48	56 612.94	56 652.46	56 632.81	56 615.57
7.5	56 729.96		56 691.99	56 607.05B	56 648.60	56 626.66	56 607.05B
8.5	56 723.82B		56 681.45	56 600.21	56 643.50		56 597.46
9.5	56 716.30		56 669.76		56 637.07		56 586.73
10.5	56 707.51		56 656.86B		56 629.24		56 574.78
11.5	56 697.35		56 642.74		56 619.88		56 561.50
12.5	56 685.73		56 627.27		56 609.06		56 546.80
13.5	56 672.62		56 610.42		56 596.56		56 530.65
14.5	56 657.99		56 592.11		56 582.42		56 512.94
15.5	56 641.81B		56 572.32		56 566.64		56 493.62
16.5	56 623.99B		56 551.01		56 549.17		56 472.66
17.5	56 604.57		56 528.11		56 529.93		56 450.00
18.5	56 583.53		56 503.66		56 508.88		
19.5	56 560.91		56 477.58		56 486.33		
20.5	56 536.67						

$\beta(14,0)$ band $[B(14)$-$X(0)]$

J	R_{11}	Q_{11}	P_{11}	R_{22}	Q_{22}	P_{22}	R_{21}
0.5	58 542.03B	58 538.97					
1.5	58 542.03B	58 536.99	58 533.96B	58 471.05	58 465.72		
2.5	58 540.78	58 533.96B	58 528.64	58 469.94	58 462.47	58 457.12	58 589.76w
3.5	58 538.20	58 529.06B	58 521.99	58 467.49	58 457.89	58 450.42	58 588.71w
4.5	58 534.31		58 514.05	58 463.70	58 452.11B	58 442.42	58 584.73w
5.5	58 529.06	58 515.95	58 504.77	58 458.60	58 444.82	58 433.09	58 579.76w
6.5	58 522.48		58 494.18	58 452.11	58 436.25	58 422.45	58 573.55w
7.5	58 514.55		58 482.25	58 444.31	58 426.29	58 410.45	58 566.64w
8.5	58 505.27		58 469.02	58 435.11	58 415.06	58 397.12	58 558.52w
9.5	58 494.65		58 454.33	58 424.53		58 382.40B	58 549.12w
10.5	58 482.61		58 438.40B	58 412.57		58 366.39	
11.5	58 469.35		58 421.05B	58 399.20		58 348.95	
12.5	58 454.49		58 402.36B	58 384.42		58 330.13	
13.5	58 438.40B		58 382.40B	58 368.22		58 309.92	
14.5	58 421.04B		58 360.94	58 350.57		58 288.40B	
15.5	58 402.36B		58 338.13	58 331.55		58 265.27B	
16.5	58 382.40B		58 313.91	58 311.05		58 240.86B	
17.5	58 360.94B		58 288.30B	58 289.15		58 214.90	
18.5	58 338.13B		58 261.43	58 265.27B		58 187.57	
19.5			58 232.89	58 240.86B		58 158.92	
20.5			58 203.59			58 128.81	

TABLE I. (*Continued.*)

(c) $\delta(2,0)$ band $[C(2)\text{-}X(0)]$

	R_{11}		P_{11}		P_{12}		R_{22}	
J	*ee*	*ff*	*ee*	*ff*	*ee*	*ff*	*ee*	*ff*
0.5	57 073.27							
1.5	57 075.46B		57 063.93B				56 979.47	
2.5	57 077.27		57 059.88B				56 981.99	
3.5	57 078.69		57 055.41B				56 984.36B	
4.5	57 079.78		57 050.52				56 986.51B	
5.5	57 080.60		57 045.26				56 988.94	56 988.61
6.5	57 081.39		57 039.66				56 991.15	56 990.55
7.5	57 081.98B		57 033.73	57 033.86			56 993.37	56 992.55
8.5	57 081.98B	57 082.60B	57 027.70	57 027.95			56 995.68	56 994.59
9.5	57 082.30b	57 083.08B	57 021.35	57 021.80B	56 896.60B	56 897.60b	56 998.12	56 996.75
10.5	57 082.60B	57 083.75B	57 015.02	57 015.70b	56 889.51B	56 890.27	57 000.64	56 999.04
11.5	57 083.08B	57 084.60B	57 008.67	57 009.59B	56 882.18	56 883.25	57 003.55B	57 001.45
12.5	57 083.75B	57 085.62B	57 002.38	57 003.55B	56 874.80	56 876.05	57 006.52	57 004.60
13.5	57 084.60B	57 086.78B	56 996.18	56 997.68	56 867.40	56 869.32	57 009.59B	57 007.10
14.5	57 085.62B	57 088.03B	56 990.17	56 991.98			57 013.58	57 010.03
15.5	57 086.78B	57 090.09	56 984.37B	56 986.51B			57 016.74	57 013.02
16.5	57 088.03B	57 091.88B	56 978.75	56 981.03			57 020.16	57 015.70B
17.5	57 089.24	57 092.97	56 973.16	56 976.52			57 023.45	57 019.21
18.5	57 090.52	57 094.53	56 967.71B	56 971.52B			57 026.44	57 021.80B
19.5	57 091.40	57 095.76	56 962.36	56 966.01B				
20.5	57 091.88B	57 096.44	56 956.80B	56 960.84				
21.5			56 951.06	56 955.43				

	P_{22}		R_{21}		P_{21}		Q_{11}	Q_{22}
J	*ee*	*ff*	*ee*	*ff*	*ee*	*ff*		
0.5							57 068.96	
1.5							57 068.26	56 971.52B
2.5	56 962.91				57 083.08B		57 067.16B	56 970.94
3.5	56 958.75B		57 104.79		57 079.24			56 969.96
4.5	56 954.48		57 107.52		57 075.46B			56 968.90
5.5	56 949.97		57 110.24		57 071.36			59 967.72B
6.5	56 945.31		57 113.19	57 112.52	57 067.66	57 067.16B		59 966.61
7.5	56 940.83	56 940.41	57 116.11	57 115.23	57 063.93B	57 063.10		
8.5	56 936.15	56 935.54	57 119.23	57 118.02	57 059.88B	57 059.03		
9.5	56 931.50	56 930.67	57 122.59	57 121.05	57 056.03	57 055.41B		
10.5	56 926.94	56 925.86	57 126.06	57 124.34	57 052.39	57 051.24		
11.5	56 922.53	56 921.16	57 130.01	57 127.80	57 049.03	57 047.52		

TABLE I. (*Continued.*)

12.5	56 918.22	56 916.60	57 134.14	57 132.14	57 045.91	57 044.14		
13.5	56 914.28	56 912.19	57 138.42	57 135.74	57 043.10	57 040.71B		
14.5	56 910.49	56 908.48	57 143.66	57 139.94	57 040.71B	57 038.55		
15.5	56 906.70	56 904.21	57 148.17	57 144.69	57 038.24	57 035.49		
16.5	56 903.94	56 900.21B	57 153.27	57 148.51	57 036.78	57 032.96B		
17.5	56 900.21B	56 896.60B	57 157.80		57 034.68	57 030.72		
18.5	56 896.60B	56 892.44			57 032.96B			
19.5	56 893.28	56 888.93						
20.5	56 889.51B	56 884.87B						
21.5	56 884.87B	56 880.06						

$\delta(3,0)$ band $[C(3)\text{-}X(0)]$

	R_{11}		P_{11}		R_{22}		P_{22}		Q_{22}
J	*ee*	*ff*	*ee*	*ff*	*ee*	*ff*	*ee*	*ff*	
0.5	59 211.05								
1.5	59 212.47		59 202.15		59 125.34B				59 118.34
2.5	59 212.96B		59 197.65		59 126.81B		59 109.58B		59 116.86
3.5	59 212.96B		59 192.38		59 127.58B		59 104.81		59 115.06B
4.5	59 211.95		59 186.30		59 127.58B		59 099.33		59 112.07
5.5	59 210.16		59 179.37B		59 126.81B		59 093.17		
6.5	59 207.46		59 171.82		59 125.34B		59 086.32		
7.5	59 203.87		59 163.33		59 122.97	59 122.68	59 078.68		
8.5	59 199.28		59 153.97		59 119.57	59 119.07	59 070.21		
9.5	59 193.69		59 143.68		59 115.06B	59 114.68	59 061.11	59 060.84	
10.5	59 186.94		59 132.44		59 109.58B	59 109.06	59 050.84	59 050.48	
11.5	59 179.37B		59 120.14		59 102.60	59 102.13	59 039.50	59 039.09	
12.5	59 169.91		59 106.74		59 094.44	59 093.81	59 027.07	59 026.55	
13.5	59 159.41		59 092.15		59 084.83	59 084.12	59 013.39	59 012.77	
14.5	59 147.49		59 076.30		59 073.71	59 073.05	58 998.32	58 997.67	
15.5	59 134.04	59 134.41	59 059.13				58 981.84	58 981.14	
16.5	59 119.20		59 040.48		59 046.37	59 045.76			
17.5			59 020.47		59 029.99	59 029.54			
18.5			58 998.78	58 999.07					

(d) $\epsilon(2,0)$ band $[D(2)\text{-}X(0)]$

J	$R_{11ee}+Q_{21fe}$	$Q_{11ef}+P_{21ff}$	P_{11ee}	P_{12ee}	R_{22ff}	$Q_{22fe}+R_{12ee}$	$P_{22ff}+Q_{12ef}$	R_{21ff}
0.5	57 808.47B	57 804.58						57 816.27
1.5	57 811.48B	57 803.48B	57 799.50	57 679.60	57 703.04	57 691.35	57 683.31B	57 822.96B
2.5	57 814.58B	57 802.93B	57 795.09	57 674.92	57 710.13	57 694.51	57 682.62B	57 830.29
3.5	57 818.59	57 802.93B	57 791.28	57 670.78	57 717.62	57 698.09	57 682.62B	57 838.06
4.5	57 822.96B	57 803.48B	57 788.00	57 667.03	57 725.56B	57 702.14	57 682.62B	57 846.37B

TABLE I. (*Continued.*)

5.5	57 828.09	57 804.58B	57 785.25	57 663.75	57 733.92	57 706.64	57 683.31B	57 855.32B
6.5	57 833.65	57 806.30	57 783.01	57 660.93	57 742.81	57 711.56	57 684.30	57 864.77
7.5	57 839.73	57 808.47B	57 781.35	57 658.52	57 752.02	57 716.95	57 685.81	57 874.68
8.5	57 846.37B	57 811.48B	57 780.06B	57 656.58	57 761.69	57 722.79	57 687.72	57 885.21
9.5	57 853.53	57 814.58B	57 779.54B	57 655.08	57 771.88	57 729.07	57 690.12	57 896.24
10.5	57 861.24	57 818.35	57 779.54B	57 654.07	57 782.53B	57 735.79	57 692.98	57 907.76B
11.5	57 869.48	57 822.70	57 780.06B	57 653.43B	57 793.52	57 742.89	57 696.28	57 919.90
12.5	57 878.23	57 827.55	57 781.04	57 653.43B	57 805.07	57 750.60	57 700.03	57 932.53
13.5	57 887.53	57 832.93	57 782.53B	57 653.43B	57 816.99	57 758.67	57 704.25	57 945.69
14.5	57 897.38	57 838.89	57 784.64	57 654.44	57 829.39	57 767.24	57 708.88	57 959.40
15.5	57 907.76B	57 845.37	57 787.26	57 655.70	57 842.28	57 776.21	57 714.01	57 973.71
16.5	57 918.56	57 852.36	57 790.35		57 855.32B	57 785.67	57 719.58	57 988.31
17.5	57 929.94	57 859.89	57 794.07			57 795.55	57 725.56B	58 003.55
18.5	57 941.84	57 867.91	57 798.23			57 805.85	57 732.11	58 019.29
19.5	57 954.24	57 876.48				57 816.64	57 738.99	58 035.45
20.5	57 967.10	57 885.53					57 746.38	
21.5	57 980.52	57 895.06					57 754.16	
22.5	57 994.24	57 905.04						
23.5	58 008.39							

$\epsilon(3,0)$ band $[D(3)\text{-}X(0)]$

J	R_{11ee} $+Q_{21fe}$	Q_{11ef} $+P_{21ff}$	P_{11ee}	P_{12ee}	R_{22ff}	Q_{22fe} $+R_{12ee}$	P_{22ff} $+Q_{12ef}$	R_{21ff}
0.5	59 991.11	59 987.26						59 998.82
1.5	59 993.81	59 986.10	59 982.26	59 862.31	59 885.27B	59 873.88	59 866.21	60 005.36
2.5	59 996.99	59 985.34B	59 977.74	59 857.60	59 892.20	59 876.83	59 865.35	60 012.38
3.5	60 000.69	59 985.34B	59 973.77	59 853.24	59 899.39	59 880.20	59 864.87B	60 019.90
4.5	60 004.90	59 985.52	59 970.25	59 849.30	59 907.04	59 883.93	59 864.87B	60 027.94
5.5	60 009.59	59 986.44	59 967.28B	59 845.80	59 914.86B	59 888.13	59 865.10	60 036.44
6.5	60 014.78	59 987.76	59 964.78	59 842.70	59 923.43	59 892.68B	59 865.79	60 045.43
7.5	60 020.41B	59 989.62	59 962.77	59 839.99	59 932.22	59 897.65	59 866.90	60 054.92
8.5	60 026.59	59 991.93B	59 961.29	59 837.66	59 941.38	59 903.00	59 868.44	60 064.87
9.5	60 033.19	59 994.71	59 960.34	59 835.78	59 950.89	59 908.72	59 870.34	60 075.27
10.5	60 040.28	59 997.98	59 959.70B	59 834.29	59 960.83B	59 914.86B	59 872.65	60 086.08
11.5	60 047.77	60 001.70	59 959.70B	59 833.12	59 970.88	59 921.26	59 875.31	60 097.33
12.5	60 055.67	60 005.85	59 960.13	59 832.46B	59 981.36	59 928.03	59 878.30	60 108.88
13.5	60 063.91	60 010.38	59 960.83B	59 831.97B	59 991.93B	59 935.05	59 881.67	60 120.66
14.5	60 072.38	60 015.29	59 962.07	59 831.97B		59 942.19	59 885.27B	60 132.39
15.5	60 080.84	60 020.41B	59 963.67	59 831.97B		59 949.25	59 889.03	
16.5	60 088.97	60 025.59	59 965.47	59 832.46B		59 956.03	59 892.68B	
17.5		60 030.31	59 967.28B					
18.5		60 034.11						

TABLE II. Observed term values of the $B(10,12,14)$, $C(2,3)$, and $D(2,3)$ levels of NO. Values followed by B are obtained from blended lines. Molecular constants are given for the $B(14)$, $D(2)$, and $D(3)$ levels. (a) The term values of the $B(10)$ and $C(1)$ levels of NO (in cm^{-1}). (b) The term values of the $B(12)$ and $B(14)$ levels of NO (in cm^{-1}). (c) The term values of the $C(2)$ and $C(3)$ levels of NO (in cm^{-1}). (d) The term values of $D(2)$ and $D(3)$ levels of NO (in cm^{-1}).

(a)

	$C(1)F_1 \rightarrow B(10)F_1$		$C(1)F_2 \rightarrow B(10)F_2$		$B(10)F_1 \rightarrow C(1)F_1$		$B(10)F_2 \rightarrow C(1)F_2$	
J	e	f	e	f	e	f	e	f
0.5	54 690.00	54 690.01			55 090.44	55 090.46		
1.5	54 692.61	54 692.63	54 699.33	54 699.35	55 093.50	55 093.53	55 138.50	55 138.50
2.5	54 700.18	54 700.19	54 711.12	54 711.12	55 098.52	55 098.55	55 143.61	55 143.61
3.5	54 711.66	54 711.70	54 726.85	54 726.54	55 105.50	55 105.55	55 150.84	55 150.84
4.5	54 727.07	54 727.08	54 746.28	54 745.82	55 114.49	55 114.55	55 160.11	55 160.11
5.5	54 746.19	54 746.66	54 769.60	54 768.94	55 125.52	55 125.59	55 171.71	55 171.71
6.5	54 769.24	54 769.88	54 796.77	54 795.88	55 138.52	55 138.60	55 185.27	55 185.27
7.5	54 796.18	54 797.02	54 827.78	54 826.64	55 153.54	55 153.63	55 200.90	55 200.91
8.5	54 826.92	54 828.00	54 862.63	54 861.22	55 170.71	55 170.81	55 218.67	55 218.67
9.5	54 861.45	54 862.82	54 901.28	54 899.58	55 189.65	55 189.76	55 238.66	55 238.67
10.5	54 899.81	54 901.47	54 943.74	54 941.71	55 210.76	55 210.88	55 260.54	55 260.55
11.5	54 941.93	54 943.91	54 989.96	54 987.56	55 233.77	55 233.89	55 284.76	55 284.76
12.5	54 987.76	54 990.09	55 039.84	55 037.08				
13.5	55 037.26	55 039.98	55 093.32	55 090.18				
14.5	55 090.36	55 093.44	55 150.25	55 146.73				
15.5	55 146.90	55 150.38	55 210.31	55 206.48	55 349.83	55 350.00		
16.5	55 206.65	55 210.46	55 273.20	55 269.04	55 385.33	55 385.51	55 441.86	55 440.81
17.5	55 269.16	55 273.25	55 337.70	55 333.63	55 424.43	55 424.62	55 481.04	55 480.18
18.5	55 333.72	55 337.88	55 402.67	55 398.79	55 468.19	55 468.39	55 526.02	55 524.50
19.5	55 398.78	55 403.22	55 465.43	55 462.66	55 517.79	55 518.54	55 578.13	55 575.47
20.5	55 461.95		55 525.58	55 523.47	55 573.65	55 575.60	55 640.36	55 635.84
21.5	55 520.96	55 522.93			55 636.21	55 640.03	55 713.33	55 706.87
22.5	55 575.88	55 577.49			55 707.39	55 713.46	55 795.22	55 787.53
23.5	55 628.74	55 630.13			55 787.85	55 795.34	55 883.94	55 875.07
24.5					55 875.29	55 883.97	55 978.09	55 968.37
25.5					55 968.57	55 978.19	56 077.07	56 066.28
26.5					56 066.74	56 077.10	56 180.38	56 168.67
27.5					56 168.94	56 180.45	56 287.78	56 275.23
28.5					56 275.43	56 287.84		
29.5					56 385.91	56 399.15		
30.5						56 514.17		

(b)

	$B(12)$				$B(14)$			
J	F_{1e}	F_{1f}	F_{2e}	F_{2f}	F_{1e}	F_{1f}	F_{2e}	F_{2f}
0.5	56 739.23	56 739.24			58 538.97	58 538.97		
1.5	56 742.91	56 742.93	56 774.37	56 774.37	58 542.00	58 542.03	58 590.62	58 590.62
2.5	56 749.00	56 749.04	56 781.26	56 781.26	58 547.05	58 547.10	58 595.97	58 595.97
3.5	56 757.54	56 757.58	56 790.88	56 790.88	58 554.15	58 554.19	58 603.45	58 603.45
4.5	56 768.44	56 768.50	56 802.98B	56 802.98B	58 563.26	58 563.32	58 613.04	58 613.04
5.5	56 781.70	56 781.77	56 817.87	56 817.88	58 574.40	58 574.48	58 624.74	58 624.74
6.5	56 797.30	56 797.38	56 835.12	56 835.12	58 587.54	58 587.63	58 638.54	58 638.54
7.5	56 815.17	56 815.26	56 854.76	56 854.76	58 602.72	58 602.81	58 654.40	58 654.41
8.5	56 835.24	56 835.34	56 876.68	56 876.68	58 619.81	58 619.92	58 672.38	58 672.38
9.5	56 857.52B	56 857.63B	56 900.81	56 900.81	58 638.97	58 639.08	58 692.41	58 692.42
10.5	56 881.76	56 881.89	56 927.02	56 927.03	58 660.05	58 660.13	58 714.48	58 714.49
11.5	56 908.08	56 908.22	56 955.26	56 955.26	58 683.17	58 683.30	58 738.59	58 738.60
12.5	56 936.36	56 936.50	56 985.43	56 985.44	58 708.37	58 708.50	58 764.73	58 764.74
13.5	56 966.53	56 966.68	57 017.51	57 017.52	58 735.30	58 735.44	58 792.85	58 792.87
14.5	56 998.55	56 998.71	57 051.36	57 051.37	58 764.35B	58 764.51B	58 823.02	58 823.03
15.5	57 032.39	57 032.57	57 086.98	57 087.00	58 795.27	58 795.45	58 855.13	58 855.15
16.5	57 067.98	57 068.16	57 124.36	57 124.38	58 828.17B	58 828.35B	58 889.26	58 889.28
17.5	57 105.36	57 105.55	57 163.49	57 163.52	58 863.11	58 863.31	58 925.34	58 925.35
18.5	57 144.44	57 144.64	57 204.25	57 204.28	58 899.75	58 899.95	58 963.45	58 963.48

TABLE II. (*Continued.*)

19.5	57 185.23	57 185.43	57 246.60	57 246.64	58 938.95B	58 939.16B	59 003.52	59 003.55
20.5	57 227.77	57 227.98	57 290.85	57 290.89			59 045.37B	59 045.40
21.5	57 272.03	57 272.25						

T_0	58 563.29(1)	
A	50.65(2)	
B	1.0381(2)	
$D\times10^4$	4.11(5)	
A_D	0.0060(2)	
p	0.012(2)	
$q\times10^4$	0.411	fixed

(c)

	$C(2)$				$C(3)$			
J	F_{1e}	F_{1f}	F_{2e}	F_{2f}	F_{1e}	F_{1f}	F_{2e}	F_{2f}
0.5	57 068.96B	57 068.96B			59 207.16	59 207.19		
1.5	57 073.28b	57 073.28B	57 096.43B	57 096.44B	59 211.03	59 211.06	59 243.26	59 243.26
2.5	57 080.47B	57 080.51B	57 104.36B	57 104.37B	59 217.46	59 217.50	59 250.37	59 250.37
3.5	57 090.63B	57 090.68B	57 115.52B	57 115.54B	59 226.41	59 226.46	59 260.36	59 260.36
4.5	57 103.75B	57 103.81B	57 129.94B	57 129.95B	59 237.94B	59 238.00B	59 273.11	59 273.11
5.5	57 119.88B	57 119.95B	57 147.66B	57 147.59B	59 252.05	59 252.12	59 288.61	59 288.62
6.5	57 139.03	57 139.24	57 168.90	57 168.51	59 268.64	59 268.72	59 306.77	59 306.77
7.5	57 161.41	57 161.76	57 193.43	57 192.84	59 287.68	59 287.77	59 327.51	59 327.51
8.5	57 186.82	57 187.37B	57 221.45	57 220.62	59 309.16	59 309.26	59 351.06	59 350.78
9.5	57 215.60	57 216.30	57 252.96	57 251.89	59 333.00	59 333.12	59 376.87	59 376.45
10.5	57 247.70	57 248.78	57 288.06	57 286.68	59 359.16	59 359.28	59 405.03	59 404.63
11.5	57 283.22	57 284.51	57 326.70	57 325.07	59 387.53	59 387.66	59 435.52	59 435.05
12.5	57 322.16	57 323.77	57 369.05	57 366.98	59 418.09	59 418.24	59 468.16	59 467.63
13.5	57 364.58	57 366.55	57 414.99	57 413.08	59 450.72	59 450.87	59 502.89	59 502.26
14.5	57 410.56B	57 412.89B	57 464.42	57 461.90	59 485.35	59 485.21	59 539.61	59 538.91
15.5	57 460.13	57 462.59	57 518.16	57 514.56	59 521.88	59 522.05	59 578.27	59 577.62
16.5	57 513.03	57 516.53	57 574.47	57 570.78	59 560.29	59 560.66		
17.5	57 569.40B	57 573.42B	57 634.57	57 631.13	59 600.52	59 600.86	59 660.69	59 660.11
18.5	57 629.17	57 633.02	57 697.74	57 693.52			59 704.31	59 703.90
19.5	57 692.21	57 696.42	57 764.16	57 759.61B				
20.5	57 758.26	57 762.83	57 833.18B	57 828.41				
21.5	57 827.24B	57 832.01						

(d)

	$D(2)$		$D(3)$	
J	F_{1e}	F_{2f}	F_{2e}	F_{2f}
0.5	57 804.52	57 808.49B	59 987.26	59 991.12B
1.5	57 808.43	57 816.28	59 991.12	59 998.82
2.5	57 816.34	57 827.95	59 998.81	60 010.37
3.5	57 828.08	57 843.67	60 010.35	60 025.73
4.5	57 843.70	57 863.18	60 025.75	60 044.95
5.5	57 863.23	57 886.58B	60 045.00	60 068.06
6.5	57 886.61	57 913.87	60 068.07	60 094.92
7.5	57 913.88	57 945.07	60 094.98	60 125.69
8.5	57 945.03	57 980.11	60 125.79	60 160.26
9.5	57 980.09	58 018.99	60 160.32	60 198.63
10.5	58 019.01B	58 061.83	60 198.65	60 240.81
11.5	58 061.84B	58 108.50B	60 240.88B	60 286.65
12.5	58 108.47B	58 159.05	60 286.78B	60 336.38
13.5	58 159.03	58 213.48	60 336.48	60 389.76
14.5	58 213.46	58 271.79	60 389.89	60 446.60
15.5	58 271.73	58 333.97	60 446.85	60 506.80
16.5	58 333.96B	58 399.99B	60 507.07B	60 570.35B
17.5	58 399.94B	58 469.87	60 570.36B	60 635.80B
18.5	58 469.83B	58 543.61	60 636.00B	
19.5	58 543.55B	58 621.18		

TABLE II. (*Continued.*)

20.5	58 621.12B	58 702.52		
21.5	58 702.49B	58 787.67B		
22.5	58 787.67B	58 876.61B		
23.5	58 876.61B	58 969.25B		
24.5	58 969.25B			
	T_0	57 804.66(2)	T_0	59 987.21(3)
	B	1.9499(2)	B	1.9284(6)
	D	$1.4(6)\times10^{-5}$	D	$5.5(3)\times10^{-5}$

therefore too low by amounts ranging from 2% to 20%. The correction described at the end of Sec. II has been applied to the cross sections of all rotational lines of all observed bands, including those previously published. The results are presented in Table III. The integrated cross sections of blended lines, followed by "*b*" in Table III, have been obtained by using branching ratios observed for other transitions together with the Boltzmann population distribution. The values listed in these tables can be divided by the fractional populations of the rotational levels to obtain values proportional to the line oscillator strengths.

The integrated cross sections of the the $\delta(0,0)$ and $\beta(7,0)$ bands are given in Table IIIa. These values supersede our earlier values,[8] because of the better experimental conditions and higher signal-to-noise ratios. The upper levels of both bands are homogeneously perturbed at very low J, and the branch lines with the F_2' level of the $\beta(7,0)$ band appear stronger than those with the F_1' level because of the stronger interaction for the F_2' level.

The results for the $\delta(1,0)$ and $\beta(10,0)$ bands are presented in Table IIIb. The intensities are affected by the interaction between the upper levels $C(1)$ and $B(10)$, as shown by the plot of the term values in Fig. 1. The two lower curves [the F_1 and F_2 components of the $C(1)$ level] are taken from our previous report[2] and the two upper curves [the F_1 and F_2 components of the $B(10)$ level] from the present work. The rotational levels of $B(10)$ with $J\geqslant13$ belong really to the extension of the $C(1)$ level. Therefore the intensities of lines with $J\geqslant13$ should be treated as belonging to the $\delta(1,0)$ band.

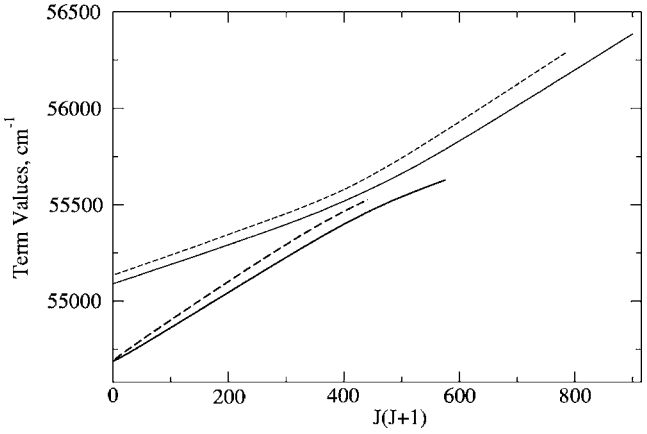

FIG. 1. The term values of the $C(1)$ and $B(10)$ levels plotted against $J(J+1)$. The solid curves are the F_1 component and the broken curves are the F_2 component. The heavy curves are the $C(1)$ level and the thin curves are the $B(10)$ levels.

The integrated cross sections of the $\beta(6,0)$, $\beta(9,0)$, $\beta(11,0)$, $\beta(12,0)$, and $\beta(14,0)$ bands are presented in Table IIIc. The $B(12)$ level, the upper level of the $\beta(12,0)$ band, is homogeneously perturbed by the $C(2)$ level, the upper level of the $\delta(2,0)$ band. The bands appear separately as two independent bands, but their separation comes from the strong interaction. The $\beta(12,0)$ band appears ten times stronger than the other β bands because of the enhancement of its intensity from the $\delta(2,0)$ band.

The integrated cross sections of the $\epsilon(v,0)$ bands with $v=0-3$ are presented in Table IIId. The results for the $\epsilon(0,0)$ and $\epsilon(1,0)$ bands supersede our earlier values.[3,6] The upper state of these bands, the $D\,^2\Sigma$ state, could interact heterogeneously with the $B\,^2\Pi$ state, but the interaction occurs at high J levels beyond our observations.

The results for the $\delta(2,0)$ and $\delta(3,0)$ bands are presented in Table IIIe. The upper levels of $C(2)$ and $C(3)$ are homogeneously perturbed by the $B(12)$ and $B(15)$ levels, respectively. The integrated cross sections of the P_{11} branch lines of the $\delta(2,0)$ and $\beta(12,0)$ bands are plotted against J'' in Fig. 2. The open diamonds and circles represent the integrated cross sections of the $\delta(2,0)$ and $\beta(12,0)$ bands, respectively. The peak intensities appear at $J\sim10$ and $J\sim5$ for the $\delta(2,0)$ and $\beta(12,0)$ bands, respectively. These shifts from the Boltzmann population distribution come from the perturbation between the $C(2)$ and $B(12)$ levels. The sum of the branch lines of both bands is plotted as the open squares in the same figure, and this represents the normal Boltzmann population.

The integrated cross sections of the $\gamma(3,0)$ band are presented in Table IIIf. These values supersede our earlier values.[4]

The uncertainties in the integrated cross sections arise from noise and the errors in the measurement of path length and pressure. For the unblended strong lines, the uncertainty due to noise is estimated to be 3%–4%, and for the weaker lines it is about 10%. The larger uncertainties of weaker lines do not significantly affect the total integrated cross section of the band, because this is determined predominantly by the strong lines. The uncertainty in the total integrated cross section for the band is estimated to be about 5%.

The band oscillator strength of a (v',v'') band is given by

$$f(v',v'')=\frac{mc^2}{\pi e^2}\frac{1}{\tilde{N}(v')}\int\sigma(\nu)d\nu, \tag{1}$$

in which $\tilde{N}(v')$ is the fractional Boltzmann population of the absorbing vibrational level—in this case since $v''=0$ this

TABLE III. Integrated cross sections of the NO bands $\beta(v,0)$ with v=6, 7,9–12,14, $\delta(v,0)$ with v=0–3, $\epsilon(v,0)$ with v=0–3, and $\gamma(3,0)$, in units of 10^{-17} cm^{-1}. Lines followed by b are blended, and intensities have been apportioned according to branching ratios. (a) Integrated cross sections of the $\delta(0,0)$ and $\beta(7,0)$ bands. (b) Integrated cross sections of the $\delta(1,0)$ and $\beta(10,0)$ bands. (c) Integrated cross sections of the $\beta(v,0)$ bands with v=6, 9,11,12, and 14. The extra line observed for the $\beta(9,0)$ band are listed under extra. (d) Integrated cross sections of the $\epsilon(v,0)$ bands with v=0–3. (e) Integrated cross sections of the $\delta(2,0)$ and $\delta(3,0)$ bands. (f) Integrated cross sections of the $\gamma(3,0)$ band.

(a) $\delta(0,0)$ band

	R_{11}		P_{11}		R_{12}		P_{12}		R_{22}		P_{22}		R_{21}		P_{21}	
J	*ee*	*ff*	*ee*	*ff*	*ee*	*ff*	*ee*	*ff*	*ee*	*ff*	*ee*	*ff*	*ee*	*ff*	*ee*	*ff*
0.5		1.37														
1.5		1.71		0.61										0.30		
2.5		2.17b		0.88b						0.67		0.51b	0.47	0.66		
3.5		2.35b		1.34					0.59	0.62b		0.60b	0.88	0.93		0.70
4.5	1.33	1.41		1.65	0.25	0.34		0.18	0.70b	0.76b		1.11	1.08b	1.08	0.63b	0.72
5.5	1.51	1.46		2.29	0.49	0.59		0.31	0.87b	0.77	0.69b	0.72b	1.12	1.12	0.68	1.00b
6.5	1.59	1.69	1.24	1.34	0.61	0.62	0.42	0.19	0.91	0.90	0.78	0.76b	1.13	1.13	0.87	1.18b
7.5	1.94b	1.93	1.35b	1.47b	0.63b	0.70	0.44	0.31	0.97b	0.93	0.81b	0.79	1.18	1.01	0.98b	1.19
8.5	1.63	1.62	1.47b	1.45b	0.58	0.71b	0.47b	0.41b	0.93	1.03	0.87	0.95	1.19	1.03b	1.00b	1.22
9.5	1.65b	1.55	1.37	1.69b	0.47	0.54	0.49b	0.51b	0.84	0.92	0.96b	1.07	1.10	0.97	0.93	1.28b
10.5	1.44b	1.37	1.38b	1.53b	0.43b	0.52	0.47b	0.51	0.78b	0.94b	0.87	1.12	1.02	0.82	0.83	1.04
11.5	1.37b	1.49	1.26b	1.54b	0.32	0.37	0.44b	0.50b	0.71	0.73	0.83	1.04	0.78	0.63	0.75	0.88
12.5	1.15	1.30	1.10b	1.29b	0.26b	0.34	0.39b	0.39	0.72b	0.65b	0.77	0.95	0.65	0.55	0.70	0.78
13.5	1.07	1.14	0.91	1.04b	0.22	0.31	0.29b	0.29	0.62	0.69b	0.70	0.89	0.52	0.46	0.67	0.71
14.5	0.95	0.95	0.86	0.87	0.20	0.22	0.25b	0.22	0.61b	0.60	0.67	0.73	0.48	0.39	0.65b	0.63
15.5	0.83	1.12	0.80	0.79	0.17	0.21	0.22b	0.15	0.48b	0.49	0.57	0.57	0.38	0.34	0.58b	0.60
16.5	0.75	0.73	0.68	0.72	0.13	0.16	0.16b	0.12	0.44	0.32	0.44	0.47b	0.29	0.22	0.50b	0.49
17.5	0.54	0.66	0.59	0.51					0.38	0.25	0.37b	0.29	0.23	0.21	0.46b	0.36
18.5	0.34	0.52	0.46b	0.41					0.35	0.21			0.21	0.19	0.37	0.31
19.5			0.37b	0.13											0.37b	
20.5			0.27													
Total	44.63		35.66		10.39		8.13		22.48		21.89		22.59		24.06	
Extended	48.59		39.06		11.35		8.90		25.08		24.72		23.66		26.16	

$\beta(7,0)$ band

J	R_{11}	P_{11}	R_{12}	R_{22}	Q_{22}	P_{22}	R_{21}	P_{21}
0.5	0.12b							
1.5	0.35b		0.16b	0.43		0.66b		1.13
2.5	0.49b	0.32	0.19b	0.66b	0.79	0.72	0.31b	1.00b
3.5	0.54	0.44	0.22b	1.03b	1.03	0.78b	0.34	0.81b
4.5	0.56	0.58		1.12	1.62	0.84b	0.37	0.59
5.5		0.50		0.73	1.32b	0.75b	0.33b	
6.5		0.43b			0.70		0.23	
7.5				0.40	0.38			
8.5					0.19			
9.5				0.16	0.13			
10.5					0.09			
11.5				0.11				
Total	2.17	2.33	0.57	4.69	3.68	6.51	3.94	1.64
Extended								

TABLE III. (*Continued.*)

	$\delta(0,0)$ band	$\beta(7,0)$ band
Total integrated cross sections (10^{-17} cm^{-1})	189.83	25.53
Total extended integrated cross sections (10^{-17} cm^{-1})	207.52	
Band oscillator strength (10^{-3})	2.34	0.288

(b)

$\delta(1,0)$ band

	R_{11}		P_{11}		Q_{11}	R_{12}		P_{12}	
J	*ee*	*ff*	*ee*	*ff*		*ee*	*ff*	*ee*	*ff*
0.5	2.01b				1.62				
1.5	3.78		1.31b			1.14b			
2.5	4.95		3.25			1.90b		0.98	
3.5	6.95b		4.45			3.31b		1.82	
4.5	6.43b	3.77	6.08b			2.61b	1.45b	2.19	
5.5	5.00	3.47b	8.66b			3.16b	1.28	2.50	
6.5	3.32b	3.90	3.65	2.83		1.78	1.22b	1.29	0.93
7.5	3.39	3.99	4.05b	3.20		1.44b	2.42b	1.31	1.12
8.5	4.01	4.96b	3.78b	2.58		1.36	1.60	1.11	1.36
9.5	3.43	4.32	3.36b	3.13b		1.17	1.41	1.20b	1.03
10.5	3.36	3.68	3.29b	2.98b		1.14b	1.29	1.30b	1.04b
11.5	3.12	3.55	2.99b	2.83b		0.84	1.00b	1.23	1.22
12.5	2.77	3.10	2.88b	2.75b		0.85	0.79	1.30	0.94b
13.5	2.55	3.28b	2.52	2.83b		0.51	0.80	1.21b	0.88b
14.5	2.26	2.75	2.38b	2.66b		0.51b	0.62	0.98b	0.71b
15.5	1.94	1.93	1.73b	2.15b		0.44	0.28		
16.5	1.58	1.88	1.23b	1.36b		0.76	0.10		
17.5	1.39	1.30b	0.98b	1.20					
18.5	0.91	0.98b	0.52			0.36b			
Total	110.01		87.61		1.62	37.18		27.65	
Extended	115.47		91.59			41.90		30.11	

$\delta(1,0)$ band

	R_{22}		P_{22}		Q_{22}	R_{21}		P_{21}	
J	*ee*	*ff*	*ee*	*ff*		*ee*	*ff*	*ee*	*ff*
0.5						1.54			
1.5	1.34				1.89	2.81			
2.5	0.62	1.49	2.65		1.27	1.98	1.76	2.77b	
3.5	1.13	2.31b	3.35			2.98	1.69b	3.24b	
4.5	1.91	1.73	3.87			1.67	2.46b	1.85	3.66
5.5	2.11	1.87b	1.87	2.13		2.58	2.42	2.78	2.26
6.5	2.16	2.35b	1.61	2.52		2.64	2.76	2.35	2.21
7.5	2.27	2.06	2.05	2.72		2.68	2.38	2.41	2.05
8.5	2.24	1.96b	1.90	2.37		2.91b	2.21	2.47	2.55b
9.5	2.17	2.37	2.00	2.12		1.99	1.62	2.05	1.38b
10.5	2.10b	3.33b	1.74b	1.88		2.07	1.86	1.80	1.63
11.5	1.90	2.08b	1.75b	1.90		1.78b	1.82b	1.42	1.09

TABLE III. (*Continued.*)

12.5	1.85	1.76	1.35b	1.60		1.64	1.43	1.57	1.23b
13.5	1.70b	1.42	1.02b	1.22		1.46	1.06	0.91	0.74b
14.5	1.35b	1.20b	2.54	0.97b		1.26	0.91	0.73	0.55b
15.5	1.24	0.47b	1.05	1.22b		0.86	0.73	0.76	0.77b
16.5			1.06	1.21				0.73b	1.02
17.5			0.49b	0.69b				0.25	0.49b
Total	52.49		52.85		3.16	57.96		49.72	
Extended	58.85		56.27			65.31		53.13	

$\beta(10,0)$ band[a]

J	R_{11}	Q_{11}	P_{11}	R_{22}	Q_{22}	P_{22}
0.5	0.019b	0.027				
1.5	0.055b	0.008	0.041b	0.033	0.055	
2.5	0.083	0.002b	0.062b	0.080b	0.033	0.035b
3.5	0.093		0.073b	0.066b	0.025b	0.029b
4.5	0.134b		0.074b	0.069	0.014	0.060
5.5	0.150b		0.065b	0.067b		0.082b
6.5	0.144b		0.075b	0.064b		0.071
7.5	0.126b		0.053b	0.062		0.062
8.5	0.098b		0.043b	0.045		0.049
9.5	0.093b		0.038b	0.030		0.038b
10.5	0.061b		0.040	0.039		0.032b
11.5	0.051b					0.032
12.5	0.043b					
Total	1.150	0.037	0.564	0.555	0.127	0.490

	R_{11}		P_{11}		R_{22}		R_{21}		P_{21}	
J	*ee*	*ff*	*ee*	*ff*	*ee*	*ff*	*ee*	*ff*	*ee*	*ff*
13.5										
14.5	0.040									
15.5	0.039									
16.5	0.090		0.045		0.036	0.027	0.028	0.011b		
17.5	0.341b		0.099		0.144b	0.051b	0.064	0.034		
18.5	0.165	0.204	0.117		0.065b	0.082	0.074	0.058b		
19.5	0.199	0.252b			0.096*	0.096	0.088b	0.061		
20.5	0.205	0.256	0.171	0.144	0.161	0.161*	0.109	0.091	0.049*	0.049
21.5	0.249	0.217	0.161	0.128	0.112*	0.112	0.111	0.079b	0.032	0.043
22.5	0.177	0.245b	0.152	0.152*	0.114	0.101b	0.079	0.063	0.078	0.078*
23.5	0.157	0.192	0.183*	0.183b	0.111b	0.111*	0.058b	0.052	0.047	0.052
24.5	0.125	0.136	0.111	0.137b	0.070	0.066	0.045	0.044	0.040	0.040*
25.5	0.078	0.115	0.089*	0.082*	0.056	0.055	0.030	0.031	0.025b	0.020b
26.5	0.082	0.078	0.067b	0.026b	0.046	0.025b	0.023	0.024	0.012b	0.013b
27.5	0.048	0.046								
28.5	0.048	0.038								
29.5	0.057b	0.028								
Total	3.907		2.938		1.898		1.257		0.578	

TABLE III. (*Continued.*)

Extended	3.918	2.998	1.933	1.283	0.619

Band	$\delta(1,0)$	$\beta(10,0)$
Total integrated cross sections(10^{-17} cm^{-1})	480.26	13.50
Total extended integrated cross sections(10^{-17} cm^{-1})	517.41	13.67
Band oscillator strength(10^{-3})	5.85	0.154

(c)

	$\beta(6,0)$ band								$\beta(9,0)$ band									
	R_{11}		P_{11}						R_{11}			P_{11}						
J	ee	ff	ee	ff	Q_{11}	R_{22}	P_{22}	Q_{22}	ee	ff	Extra	ee	ff	Extra	Q_{11}	R_{22}	P_{22}	Q_{22}
0.5		0.064			0.040					0.173b				0.112				
1.5		0.079		0.040	0.020	0.035		0.034		0.323b			0.171		0.041	0.164	0.219	
2.5		0.118		0.055		0.043	0.014	0.020		0.450			0.382b		0.000	0.259	0.147b	0.224
3.5		0.120		0.072		0.037	0.036			0.514			0.537b			0.296	0.266	0.081b
4.5	0.079	0.065		0.088		0.041	0.022			0.621			0.572b			0.421	0.258	0.069
5.5	0.064	0.055		0.087		0.060	0.050			0.613b	0.062b		0.696			0.384	0.309	0.057
6.5	0.078	0.053	0.060	0.038		0.055	0.052			0.614	0.090b		0.642			0.372	0.430	0.044
7.5	0.061	0.046	0.065	0.047		0.044	0.056			0.517	0.155b		0.471	0.044		0.411	0.342	0.018
8.5	0.052	0.053	0.057	0.043		0.070	0.061			0.567			0.570	0.054b		0.504	0.347	0.013
9.5	0.055	0.054	0.048	0.044		0.064	0.065			0.715			0.440	0.120		0.415	0.358	
10.5	0.050	0.040	0.054	0.032		0.054	0.060		0.570	0.118			0.700			0.294	0.466	
11.5	0.042	0.048	0.030	0.029		0.052	0.035		0.501	0.098			0.680			0.264	0.347	
12.5	0.030	0.042	0.042	0.026		0.051	0.025		0.413	0.090b		0.343	0.094			0.212	0.304b	
13.5	0.032	0.032	0.031	0.030		0.038	0.010		0.373	0.071		0.345	0.048			0.169	0.309b	
14.5	0.021	0.019	0.027	0.029		0.036			0.204	0.076		0.288	0.058			0.152	0.226b	
15.5	0.013	0.023	0.029	0.021		0.014			0.216	0.068		0.220	0.069			0.107b	0.187b	
16.5	0.012	0.017							0.175	0.057		0.189	0.051			0.084b	0.166b	
17.5									0.122	0.054		0.104	0.066			0.065b	0.128b	
18.5									0.096	0.040		0.097	0.040			0.046b	0.085	
19.5									0.065	0.038		0.126	0.014			0.049b		
20.5									0.055	0.028		0.065	0.017			0.025b		
21.5									0.068	0.008						0.013		
22.5									0.025	0.028								
23.5									0.015	0.011								
Total		1.517		1.124	0.060	0.693	0.486	0.054		9.097			8.313		0.153	4.706	4.675	0.725
Extended		1.667		1.262		0.801	0.527			9.370			8.684			4.916	4.841	

	$\beta(11,0)$ band						$\beta(12,0)$ band							$\beta(14,0)$ band					
J	R_{11}	P_{11}	Q_{11}	R_{22}	P_{22}	Q_{22}	R_{11}	Q_{11}	P_{11}	R_{12}	R_{22}	Q_{22}	P_{22}	R_{11}	Q_{11}	P_{11}	R_{22}	Q_{22}	P_{22}
0.5	0.24b		0.12				1.39	0.31						0.18b	0.09				
1.5	0.40b	0.25	0.04	0.21		0.23	3.09b	0.34	1.37		0.85	1.78		0.23b	0.04	0.27	0.12	0.18	
2.5	0.61	0.45		0.23	0.21b	0.17	3.97b	0.12	2.82	0.02b	1.32b	1.11	1.30	0.32	0.02b	0.36	0.18	0.12	0.12
3.5	0.67	0.57		0.36	0.29b	0.15b	4.00	0.07	4.06b	0.04b	2.05b	1.04	2.00	0.39	0.02b	0.46	0.23	0.09	0.17
4.5	0.84	0.71		0.48	0.40b	0.10	4.38	0.03	4.16	0.04b	3.04b	0.62	2.25	0.42b	0.01b	0.49	0.28	0.11b	0.22
5.5	0.89	0.75		0.49b	0.42b		4.78		5.18	0.06b	3.02	0.36	2.77b	0.49b	0.00	0.56	0.24	0.04	0.25

TABLE III. (*Continued.*)

6.5	0.85	0.84		0.47b	0.40b		4.28		5.11	0.08	3.13	0.30	2.90	0.50b		0.56	0.29b	0.04	0.27
7.5	0.84	0.84		0.50b	0.40b		4.18		4.82	0.12b	3.24	0.22	3.17b	0.50		0.61	0.27	0.04	0.28
8.5	0.82	0.84		0.49b	0.44b		4.16b		4.39	0.09	3.09		2.84	0.48		0.62	0.24	0.01	0.26
9.5	0.73	0.81		0.45b	0.39		3.58		4.04		3.02		2.98	0.45		0.50	0.23		0.25b
10.5	0.74	0.74		0.38b	0.33		3.43		3.74b		2.49		2.72	0.42		0.51b	0.22		0.22
11.5	0.61	0.65		0.37b	0.35		2.60		3.07		1.83		2.41	0.35		0.46b	0.18		0.19
12.5	0.42	0.55		0.31	0.30		2.29		2.79		1.62		1.93	0.29		0.39b	0.14		0.18
13.5	0.39	0.41		0.27	0.22		2.02		2.25		1.24b		1.73	0.26b		0.29b	0.13		0.15
14.5	0.27	0.34		0.17			1.63		2.03		1.30		1.35	0.21b		0.25b	0.10		0.14b
15.5	0.23	0.29		0.12			1.14b		1.52		1.05		1.09	0.08b		0.22b	0.09		0.11b
16.5	0.13	0.23					1.03b		1.01		0.66		0.83	0.04b		0.15	0.08		0.10b
17.5		0.15					0.67		0.74		0.33		0.32	0.03b		0.14b	0.03		0.09
18.5							0.69		0.54		0.25			0.02b		0.11	0.02b		0.07
19.5							0.26		0.32		0.22					0.06	0.01b		0.06
20.5							0.18									0.04			0.04
Total	9.68	9.42	0.16	5.30	4.15	0.65	53.45	8.70	53.96	0.45	32.75	5.43	33.59	5.67	0.18	7.03	3.08	0.62	3.17
Extended	10.15	9.88		5.78	4.53		55.70		56.25	0.62	33.62		36.04	5.92		7.30	3.23		3.39

Band	$\beta(6,0)$	$\beta(9,0)$	$\beta(11,0)$	$\beta(12,0)$	$\beta(14,0)$
Total integrated cross sections (10^{-17} cm^{-1})	3.94	27.67	29.36	188.33	19.73
Total extended integrated cross sections (10^{-17} cm^{-1})	4.37	28.69	31.15	196.36	20.63
Band oscillator strength (10^{-3})	0.049	0.324	0.352	2.22	0.233

				$\epsilon(0,0)$ band				
J	$R_{11}+Q_{21}$	P_{11}	$R_{12}+Q_{22}$	P_{12}	R_{22}	$P_{22}+Q_{12}$	R_{21}	$P_{21}+Q_{11}$
0.5	1.06							0.44
1.5	1.66b	0.36	0.89	0.97	0.10	1.60	0.62	0.61
2.5	2.35	0.70	1.31	1.07	0.74	1.64b	0.97	3.18
3.5	3.06	0.94	2.25	0.87	0.47	2.10b	1.05	3.90
4.5	3.24	1.34	2.18	1.67	0.68	1.59	0.96	3.07
5.5	3.35	1.71	2.34	1.44	1.00	2.50	1.19	3.49b
6.5	3.77	1.45	2.33	1.33	1.02	2.41	1.29	3.51
7.5	3.70	1.65	2.36	1.13	0.83b	2.17	1.36	4.33
8.5	3.87	1.60b	2.34	0.80b	0.87b	2.22	1.62	4.13b
9.5	3.71	1.31b	2.45	0.89b	0.88b	2.21	1.39	3.70b
10.5	3.26	0.98	2.80	0.61b	0.70b	1.99	0.92	3.46
11.5	3.21	1.05	2.04	0.48b	0.58	1.75	0.98b	3.16
12.5	2.71b	0.95	1.65	0.27b	0.54b	1.50	0.89	2.84
13.5	2.51	1.01b	1.47		0.45	1.33	0.85	2.63
14.5	1.99	0.89	1.54b		0.64	0.97	0.62	2.50
15.5	1.66	0.65	1.13		0.45b	0.87	0.42	2.02b
16.5	1.33b	0.60	0.80		0.52	0.80	0.20b	1.61
17.5	1.12	0.34b	0.42		0.16b	0.93		1.32
18.5	1.04	0.28b	0.53			0.45		0.95
19.5	0.83	0.21b	0.47			0.47b		0.98
20.5	0.73		0.30					0.68
21.5	0.36b		0.22					0.73

TABLE III. (*Continued.*)

22.5								0.56b
Total	50.52	18.02	31.82	11.53	10.63	29.50	14.33	53.80
Extended	52.51	18.89	33.52	12.25	11.53	31.11	15.48	56.56

$\epsilon(1,0)$ band

J	$R_{11}+Q_{21}$	P_{11}	$R_{12}+Q_{22}$	P_{12}	R_{22}	$P_{22}+Q_{12}$	R_{21}	$P_{21}+Q_{11}$
0.5	1.47						1.09	1.16b
1.5	2.50	0.85b	1.06b	0.90	0.20b	1.54b	1.17b	1.95b
2.5	2.80	1.14b	1.68b	0.95	0.43	2.30b	1.72b	3.89b
3.5	3.25	1.64b	1.98	1.20	0.80b	2.66b	1.70	4.01b
4.5	3.34b	2.14b	2.23	1.01	1.01	2.85b	1.73	3.67b
5.5	3.64	2.61b	2.49	1.10	1.07	2.97b	2.22b	3.80
6.5	4.02	2.40b	2.67	1.00	1.21	2.69b	2.05	3.83
7.5	3.89	2.42b	2.85b	0.98	1.09	2.52	1.88	3.15b
8.5	3.88	2.35b	2.57	0.92	0.81	2.35	1.03	3.83
					0.61		0.85	
9.5	2.58	2.31b	1.69	0.68b	1.39	2.54b	2.19	3.87b
	2.08b		1.21					
10.5	3.72	2.23b	2.61	0.63b	1.31b	1.85b	1.70	2.91
						1.13		1.97
11.5	3.34	1.41b	2.44	0.33b	1.14	2.03	1.28	4.47
		0.58		0.20b				
12.5	3.30	1.70b	2.33	0.42b	1.09b	1.91b	1.14b	4.11b
13.5	3.26	1.85b	1.90	0.33b	1.02	1.70	0.98	3.11
14.5	2.72	1.07b	1.80	0.34	0.87	1.40	0.98	2.72
15.5	2.71	1.01b	1.60b	0.18	0.77	1.08	0.69	2.46
16.5	2.33	0.87b	1.17	0.23	0.77	0.83	0.66	2.02
17.5	1.86b	0.55b	0.99b	0.12	0.79	0.82		1.36
18.5	0.77	0.57b		0.07		0.50		1.34
19.5		0.54						0.93
20.5		0.54b						
Total	57.46	30.78	35.27	11.59	16.38	35.67	25.06	60.56
Extended	63.89	32.94	39.92	12.88	18.54	39.66	29.01	65.89

$\epsilon(2,0)$ band

J	$R_{11}+Q_{21}$	P_{11}	$R_{12}+Q_{22}$	P_{12}	R_{22}	$P_{22}+Q_{12}$	R_{21}	$P_{21}+Q_{11}$
0.5	2.15b						0.51	1.35
1.5	2.65b	1.29	0.89	0.84	0.11		1.36b	1.98b
2.5	3.05b	1.43	1.42	0.97	0.52	2.32b	1.45	2.63b
3.5	3.56	1.58	2.04	1.10	0.61	2.47b	1.79	3.17b
4.5	3.70b	1.88	2.21	1.17	0.73b	2.73b	2.39b	3.58b
5.5	4.01	1.87	2.75	1.18	1.05	2.85b	2.07b	4.06b
6.5	4.13	1.88	2.94	1.19	1.11	2.93	1.88	4.91
7.5	4.33	1.83	2.90	1.00	1.09	2.94	2.10	5.64b
8.5	4.55b	2.25b	2.82	1.11	1.21	3.01	2.05	5.28b
9.5	4.35	2.21b	2.73	0.95	1.17	2.73	1.76	5.12b
10.5	3.57	2.12b	2.58	0.82	1.17b	2.35	2.11b	4.11

TABLE III. (*Continued.*)

11.5	3.32	2.00b	2.44	0.73b	1.06	2.38	1.61	3.71
12.5	3.00	1.52	2.21	0.60b	1.04	1.75	1.52	3.80
13.5	2.75	1.50b	1.73	0.48b	0.89	1.88	1.31	3.26
14.5	2.33	1.44	1.73	0.35	0.81	1.39	1.16	2.96
15.5	2.81b	1.18	1.50	0.23	0.67	1.01	0.92	2.32
16.5	2.37	0.90	1.21		0.58b	0.83	0.81	2.56
17.5	1.74	0.82	1.15			0.83b	0.68	2.27
18.5	1.29	0.65	1.11			0.74	0.57	1.67
19.5	1.30		0.93			0.56	0.51	1.33
20.5	0.98					0.46		0.78
21.5	0.98					0.19		0.78
22.5	0.86							0.72
23.5	0.86							
Total	63.64	28.35	37.29	12.72	13.82	36.29	27.36	68.90
Extended	67.83	32.92	41.14	13.88	15.98	37.90	29.67	73.31

$\epsilon(3,0)$ band

J	$R_{11}+Q_{21}$	P_{11}	$R_{12}+Q_{22}$	P_{12}	R_{22}	$P_{22}+Q_{12}$	R_{21}	$P_{21}+Q_{11}$
0.5	0.49						0.25	0.66
1.5	1.02	0.12	0.36	0.36	0.21b	0.44	0.52	1.00
2.5	0.94	0.32	0.65	0.37	0.38b	0.72b	0.62	1.08b
3.5	1.05	0.79	0.67	0.42	0.54	0.77b	0.67	1.24b
4.5	1.27	0.53	1.13	0.41	0.41	0.81b	0.74	1.35b
5.5	1.17	0.67b	0.90	0.43	0.68b	0.84b	0.68	1.45b
6.5	1.27	0.72	1.25b	0.47	0.49	0.85	0.65	1.43
7.5	1.62b	0.78	1.13	0.36	0.49	0.88	0.61	1.34
8.5	1.43	0.53	0.97	0.37	0.69	0.90	0.57	1.25b
9.5	1.23b	0.74b	0.99	0.33	0.56	0.83	0.62	1.21
10.5	1.22	0.71b	0.95b	0.28	0.54b	0.85	0.52	1.47
11.5	1.19	0.68b	0.90	0.26	0.63	0.65	0.52	1.32
12.5	1.19	0.61b	0.85	0.26b	0.29	0.86	0.41	1.19
13.5	0.96	0.41b	0.77	0.20b	0.14b	0.68	0.36	1.26
14.5	1.06	0.42	0.80	0.15b		0.47b	0.35	0.84
15.5	0.77	0.39	0.54	0.12b		0.38		0.84b
16.5	0.36	0.28	0.43b	0.09b		0.15b		0.85
17.5			0.20b					0.50
18.5								0.43
Total	17.05	8.90	13.29	4.88	6.05	11.08	8.09	20.71
Extended	21.82	9.79	16.10	6.84	7.18	13.10	10.24	22.70

Band	$\epsilon(0,0)$	$\epsilon(1,0)$	$\epsilon(2,0)$	$\epsilon(3,0)$
Total integrated cross sections (10^{-17}cm^{-1})	220.15	272.77	288.37	78.97
Total extended integrated cross sections (10^{-17}cm^{-1})	231.85	302.73	312.63	104.64
Band oscillator strength (10^{-3})	2.62	3.42	3.53	1.22

TABLE III. (*Continued.*)

	$\delta(2,0)$ band																	
	R_{11}			P_{11}			P_{12}		R_{22}			P_{22}						
J	ee	ff	Q_{11}	ee		R_{12}	ff		ee	ff	Q_{22}	ee	ff		ee	ff		
0.5	1.66		0.30															
1.5	2.29b		0.25						0.52	0.29b								
2.5	2.82			0.67b					0.73b		0.44	0.71						
3.5	3.06			1.65b					0.95		0.54	1.02b						
4.5	3.66			2.28					1.74		0.57	1.90b						
5.5	4.25			2.84					0.88	0.92	0.29b	2.18						
6.5	4.72			2.40					1.13	1.03	0.12b	2.32						
7.5	5.22			4.08					1.28	1.12		1.35	1.24					
8.5	2.73b	2.63b		2.31	2.28				1.35	1.23		1.49	1.32					
9.5	2.46	2.79b		2.32	2.50b		0.18b	0.20	1.35	1.26		1.42	1.34					
10.5	2.56b	2.60b		2.25	2.45b		0.23b	0.27	1.24	1.18		1.35	1.40					
11.5	2.41b	2.35b		2.22	2.43b		0.31	0.33	1.21b	1.13		1.33	1.31					
12.5	2.01b	2.14b		1.99	2.31b		0.47	0.31	1.03	1.05		1.14	1.15					
13.5	1.69b	2.00b		1.75	1.88		0.40	0.07	0.82b	0.97		1.09	1.05					
14.5	1.61b	1.87b		1.53	1.71				0.62	0.75		0.98	1.03					
15.5	1.19b	1.67		1.42b	1.54b				0.54	0.44		0.75	0.94					
16.5	1.08b	1.19b		1.27	1.14				0.49	0.36b		0.68	0.74b					
17.5	0.83	1.02		1.08	0.83				0.41	0.29		0.50b	0.68b					
18.5	0.73	0.93		0.99b	0.72b				0.28	0.15b		0.49b	0.49					
19.5	0.52	0.76		0.58	0.43b							0.33	0.35					
20.5	0.31	0.26		0.47b	0.27							0.29b	0.32b					
21.5				0.33								0.22b	0.22					
Total	70.02		0.55	54.92		6.24a	2.77		28.45		2.25	35.12						
Extended	74.27			57.42			3.45		30.22			36.91						

	$\delta(2,0)$ band				$\delta(3,0)$ band													
	R_{21}		P_{21}				R_{22}			P_{22}								
J	ee	ff	ee	ff	R_{11}	P_{11}			Q_{22}	ee	ff		ee	ff				
0.5					0.67													
1.5					1.40	0.88	0.72b		0.93									
2.5					2.06b	1.46	1.06b		0.57	0.69b								
3.5	0.77		0.15		2.38b	1.69	1.22b		0.30b	0.89								
4.5	0.87		0.50b		2.78	2.07	1.34b		0.27	1.35								
5.5	1.09		0.72		2.60	2.57b	1.43b			1.45								
6.5	0.65	0.65	1.31		3.08	2.64	1.58b			1.46								
7.5	0.83	0.72	0.90	0.87	2.57	2.73	0.78	0.90		1.63								
8.5	0.88	0.89	0.93b	0.99	2.99	3.04	0.82b	0.92b		1.38								
9.5	0.98	1.00	0.87	1.01b	2.35	2.17	0.72b	0.82b		0.77	0.93							
10.5	0.91	1.04	0.80	0.85	2.06	2.52	0.60b	0.89b		0.40	0.76							
11.5	0.86	0.98	0.73	0.76	2.00b	1.76	0.56	0.77		0.42	0.61							
12.5	0.76	0.87	0.61	0.64	1.62	1.68	0.34	0.40		0.50	0.48							
13.5	0.52	0.48	0.49	0.54b	1.30	1.50	0.49	0.52		0.45	0.41							

TABLE III. (*Continued.*)

14.5	0.27	0.30	0.42b	0.44	0.88	1.28	0.20	0.27	0.21	0.35
15.5	0.26	0.29	0.23	0.36	0.81	1.04	0.27	0.20	0.27	0.17
16.5	0.16	0.08	0.19	0.30b	0.60b	0.43	0.17	0.24		
17.5	0.08		0.12	0.19		0.54	0.06	0.19		
18.5						0.50				
Total	17.19		15.92		32.15	30.50	18.48	2.07	15.58	
Extended	19.68		16.42		34.94	32.02	19.72		17.18	

Band	$\delta(2,0)$	$\delta(3,0)$
Total integrated cross sections (10^{-17} cm^{-1})	233.13	98.78
Total extended integrated cross sections (10^{-17} cm^{-1})	347.11	105.93
Band oscillator strength (10^{-3})	2.79	1.20

(f)

J	$R_{11}+Q_{21}$	P_{11}	$R_{12}+Q_{22}$	P_{12}	R_{22}	$P_{22}+Q_{12}$	R_{21}	$P_{21}+Q_{11}$
1.5	0.150	0.051	0.092	0.077	0.018	0.132	0.079	0.108
2.5	0.243	0.102	0.133	0.089	0.031b	0.187	0.108	0.231
3.5	0.281	0.140	0.171	0.095	0.047	0.194	0.123	0.303
4.5	0.315	0.146	0.209	0.096	0.068	0.230	0.147	0.339
5.5	0.349	0.171	0.221	0.092	0.080	0.257	0.160	0.371
6.5	0.356	0.178	0.246	0.095	0.088	0.261	0.163	0.426
7.5	0.398	0.212b	0.254	0.093	0.098	0.251	0.140	0.405
8.5	0.367	0.199	0.248	0.079	0.100	0.246	0.126	0.410
9.5	0.366	0.200	0.241	0.069	0.098	0.242	0.124	0.405
10.5	0.355	0.199b	0.238	0.065	0.093b	0.212	0.103	0.388
11.5	0.349	0.180b	0.212	0.057	0.092	0.194	0.090	0.376
12.5	0.314	0.140	0.202	0.048b	0.079	0.171	0.082	0.357
13.5	0.284	0.131b	0.173	0.043b	0.078b	0.162	0.069	0.313
14.5	0.253	0.126	0.145	0.034b	0.067b	0.126	0.069	0.306
15.5	0.218	0.110	0.132	0.035	0.049	0.094	0.040	0.257
16.5	0.147	0.086	0.110	0.022	0.041	0.082	0.036	0.224
17.5		0.067	0.078	0.013	0.030b	0.055	0.033	0.186
18.5		0.070	0.066		0.030	0.055	0.022	0.162
19.5						0.036	0.027b	0.120
20.5						0.026		0.101
21.5						0.021		0.072
22.5								0.051
23.5								0.020
Total	4.745	2.508	3.171	1.102	1.187	3.234	1.741	5.931
Extended	5.725	2.729	3.326	1.190	1.401	3.338	1.804	6.256

Total integrated cross sections(10^{-17} cm^{-1})	23.62
Total extended integrated cross sections(10^{-17} cm^{-1})	25.77
Band oscillator strength10^{-3}	0.291

[a]Intensities marked with * are overlapped with saturated lines of the $\delta(1,0)$ band, and values are estimated.

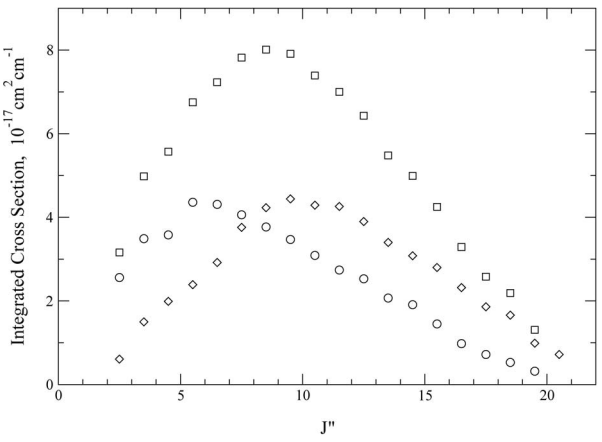

FIG. 2. Effects of the homogeneous perturbation on intensity distribution. P_{11} branch lines of the $\delta(2,0)$ and $\beta(12,0)$ bands are presented by diamonds and circles, respectively. Sum of the both bands are given by squares. The branch lines do not follow by Boltzmann distribution, but the sum of them followed.

quantity is unity—and the integration of the cross section $\sigma(\nu)$ is performed over all of the rotational lines. The total integrated cross sections of observed lines for each branch are presented as "Total" in Table III. Observations of the rotational lines are mostly limited to $J \leqslant 20.5$. The effects from higher J lines cannot be ignored. The contribution of these higher J lines was obtained by extrapolating the cross sections up to $J=36.5$ by fitting the experimental points to a Boltzmann distribution curve, as shown in Fig. 4 of Ref. 6. The results of the extended contributions are also listed in Table III as "Extended." The total integrated cross sections and band oscillator strength of each band are presented at the bottom of each table.

The band oscillator strengths of the NO bands determined by the FTS measurements are compared with those of previous measurements in Table IV. The uncertainty in our measured band oscillator strength is estimated to be about 5%, which includes uncertainties from line intensity measurements and extrapolation. The value under FTS/PB are our published values[1–6] without any correction on the integrated cross sections. The value under FTS/CR are the results after intensity correction. The ratio of those values should not be constants, because the ratio depends on the observed optical depth. Our values, obtained by line-by-line integration, are all for single bands. In the cases of the $\delta(0,0)$ and $\delta(1,0)$ bands, the values for $\beta(7,0)$ and $\beta(10,0)$, respectively, should be added for comparison with other work.

Bethke[14] measured integrated cross sections of pressure-broadened NO and gives a maximum error of 10% for his band oscillator strengths. His values agree well with ours, within the combined uncertainties, except for the $\epsilon(1,0)$ and $\gamma(3,0)$ bands. Cieslik[28] obtained the band oscillator strength by two methods, extrapolation to zero pressure and use of the

TABLE IV. Band oscillator strength (10^{-3}) of NO.

Band	Upper level	FTS					Cieslik[f]						
		CR[a]	PB[b]	LC[c]	CCB[d]	GL[e]	B	C	Beth.[g]	CP[h]	LGTM[i]	BEL[j]	MCY[k]
$\gamma(3,0)$	$A(3)$	0.291	0.269	0.30	0.356		0.30	0.308	0.360				
$\beta(6,0)$	$B(6)$	0.049	0.048		0.037				0.0462				
$\delta(0,0)$	$C(0)$	2.34			2.29	3.52	2.5	2.84	2.49	5.6	2.4	2.0	2.2
$\beta(7,0)$	$B(7)$	0.288			0.375								
$\epsilon(0,0)$	$D(0)$	2.62	2.47	1.87	2.63	2.51	2.6	2.53	2.54	2.54			
$\beta(9,0)$	$B(9)$	0.324	0.265		0.314		0.37	0.356	0.358				
$\delta(1,0)$	$C(1)$	5.85	5.4		6.01	8.53	6.0	5.63	5.78				
$\beta(10,0)$	$B(10)$	0.154											
$\epsilon(1,0)$	$D(1)$	3.42	2.88	3.75	4.61	4.60	5.6	6.46	4.60				
$\beta(11,0)$	$B(11)$	0.352	0.344		0.648				0.362				
$\beta(12,0)$	$B(12)$	2.22			2.09	2.17			2.31				
$\delta(2,0)$	$C(2)$	2.79			3.08	2.94			2.74				
$\epsilon(2,0)$	$D(2)$	3.53		3.16	3.67	3.16			3.32				
$\beta(14,0)$	$B(14)$	0.233			0.354				0.201				
$\delta(3,0)$	$C(3)$	1.20			0.976								
$\beta(15,0)$	$B(15)$				0.870								
$\epsilon(3,0)$	$D(3)$	1.22		1.44	1.79								

[a]Present works after intensity correction.
[b]Our published works (Refs. 1–6).
[c]Luque and Crosley (1999) (Ref. 17).
[d]Chan, Cooper, and Brion (1993) (Ref. 16).
[e]Guest and Lee (1981) (Ref. 15).
[f]Cieslik (1977) (Ref. 28): (B) extrapolated to zero; (C) the curve of growth.
[g]Bethke (1959) (Ref. 14).
[h]Callear and Pilling (1970) (Ref. 29).
[i]Lewis *et al.* (1989) (Ref. 30).
[j]Brzozowski *et al.* (1976) (Ref. 31).
[k]Mandelman *et al.* (1973) (Ref. 32).

curve of growth, shown in Table IV under B and C, respectively. His values agree with ours except that his values for the $\epsilon(1,0)$ are larger. Guest and Lee[15] measured integrated cross sections with a resolution of 0.03 nm, but hold the optical density below 0.4. They estimate uncertainty of 40% because the transition saturates even at low pressure. Chan *et al.*[16] observed the NO electronic spectra by using the dipole (e,e) method of electron-impact excitation, which is free of optical instrumental function and saturation errors. However, their resolution (0.048 eV, 387 cm^{-1}, or 1.26 nm at 180 nm) is not high enough to separate the band structures. They claimed the uncertainties of their measurements to be 5%–10% for strong and partially resolved bands, with additional errors expected from the deconvolution. Their values agree reasonably well with ours except for the $\epsilon(1,0)$ band and the last four bands in Table IV, $\beta(14,0)$, $\delta(3,0)$, and $\epsilon(3,0)$, together with $\beta(15,0)$, for which we did not make measurements. The large difference for the $\epsilon(3,0)$ band might be attributable to their deconvolution. The calculated values of Luque and Crosley[17] are also included in Table IV, but they normalized to different lifetimes for the γ band and the ϵ bands. Their values for the ϵ bands agree well with ours, including that for the $\epsilon(1,0)$ band, for which the values of the other measurements are much higher.

The line oscillator strengths could in principle be deduced from the band oscillator strengths using Hönl-London factors and the Boltzmann distribution. However, most of the upper levels of the NO bands are to some extent perturbed, homogeneously or heterogeneously. Consequently, as demonstrated in Fig. 2, the line intensities do not follow the Boltzmann distribution. This is especially the case for the strongly perturbed bands $\delta(2,0)$ and $\delta(3,0)$ and their partners. Therefore the actual measured integrated cross sections of the rotational lines become very important. The values presented here are for 295 K, but they could be applied to any other temperature by dividing by the rotational population at 295 K.

IV. SUMMARY

This is the final report of the FTS/PF work. We have presented lists of the observed line positions and the term values for all bands observed except those published previously,[1–7] together with their integrated cross sections. Line intensities for the bands in these previous publications have been corrected for instrumental effects, and the revised integrated cross sections are given here. The band oscillator strengths of all bands observed in this work are presented and compared with other published results. They are also provided after instrumental corrections.

ACKNOWLEDGMENTS

This work was supported in part by a NSF Division of Atmospheric Sciences Grant No. ATM-94-22854 to Harvard College Observatory and by the NASA Upper Atmospheric Research Program under Grant No. NAG5-484 to the Smithsonian Astrophysical Observatory. We also acknowledge the Paul Instrument Fund of the Royal Society for the development of the vuv-FT spectrometer. The FTS measurements at the Photon Factory were made with the approval of the Photon Factory Advisory Committee (94G367). We thank Dr. Stark for the computation program for the correction of the line integrated cross sections. One of the authors (K.Y.) thanks the Japan Society for the Promotion of Science for support. Another author (A.P.T.) thanks NATO for its Grant for international collaboration in research (890224)

[1] K. Yoshino, J. R. Esmond, W. H. Parkinson *et al.*, J. Chem. Phys. **109**, 1751 (1998).
[2] T. Imajo, K. Yoshino, J. R. Esmond *et al.*, J. Chem. Phys. **112**, 2251 (2000).
[3] J. Rufus, K. Yoshino, J. R. Esmond, A. P. Thorne, T. Imajo, K. Ito, and T. Matsui, J. Chem. Phys. **115**, 3719 (2001).
[4] A. S.-C. Cheung, D. H.-Y. Lo, K. W.-S. Leung, K. Yoshino, A. P. Thorne, J. E. Murray, K. Ito, T. Matsui, and T. Imajo, J. Chem. Phys. **116**, 155 (2002).
[5] J. Rufus, K. Yoshino, A. P. Thorne, J. E. Murray, T. Imajo, K. Ito, and T. Matsui, J. Chem. Phys. **117**, 10621 (2002).
[6] A. S.-C. Cheung, A. L. Wong, D. H.-Y. Lo, K. W.-S. Leung, K. Yoshino, A. P. Thorne, J. E. Murray, K. Ito, T. Matsui, and T. Imajo, J. Chem. Phys. **119**, 8373 (2003).
[7] A. P. Thorne, J. Rufus, K. Yoshino, A. S.-C Cheung, and T. Imajo, J. Chem. Phys. **122**, 179901 (2005).
[8] J. E. Murray, K. Yoshino, J. R. Esmond, W. H. Parkinson, Y. Sun, A. Dalgarno, A. P. Thorne, and G. Cox, J. Chem. Phys. **101**, 62 (1994).
[9] G. Herzberg, A. Lagerqvist, and E. Miescher, Can. J. Phys. **34**, 622 (1956).
[10] A. Lagerqvist and E. Miescher, Helv. Phys. Acta **31**, 221 (1958).
[11] R. Gallusser and K. Dressler, J. Chem. Phys. **76**, 4311 (1982).
[12] M. Raoult, J. Chem. Phys. **87**, 4736 (1987).
[13] V. D. Braun, K. P. Huber, and M. Verloet, J. Mol. Spectrosc. **203**, 65 (2000).
[14] G. W. Bethke, J. Chem. Phys. **31**, 662 (1959).
[15] J. A. Guest and L. C. Lee, J. Phys. B **14**, 3401 (1981).
[16] W. F. Chan, G. Cooper, and C. E. Brion, Chem. Phys. **170**, 111 (1993).
[17] J. Luque and D. R. Crosley, J. Phys. Chem. **111**, 7405 (1999).
[18] E. Mayor, A. M. Velasco, and I. Martin, J. Chem. Phys. **123**, 114305 (2005).
[19] J. W. Brault (private communication).
[20] P. M. Dooley, B. R. Lewis, S. T. Gibson *et al.*, J. Chem. Phys. **109**, 3856 (1998).
[21] R. D. Hudson and V. L. Carter, J. Opt. Soc. Am. **58**, 227 (1968).
[22] G. Stark, K. Yoshino, P. L. Smith, K. Ito, and W. H. Parkinson, Astrophys. J. **369**, 574 (1991).
[23] H. Lefebvre-Brion and R. W. Field, *The Spectra and Dynamics of Diatomic Molecules* (Elsevier, San Diego, 2004).
[24] E. Miescher (private communication).
[25] C. Amiot, R. Bacis, and G. Guelachvili, Can. J. Phys. **56**, 251 (1978).
[26] Ch. Jungen and E. Miescher, Can. J. Phys. **46**, 987 (1968).
[27] R. Engleman, Jr. and P. E. Rouse, J. Mol. Spectrosc. **37**, 240 (1971).
[28] S. Cieslik, Ci. Sci. Acad. Roy. Belg. **63**, 884 (1977).
[29] A. B. Callear and M. J. Pilling, Trans. Faraday Soc. **66**, 1886 (1970).
[30] B. R. Lewis, S. T. Gibson, L. W. Torop, and D. G. McCoy, Geophys. Res. Lett. **25**, 2457 (1998).
[31] J. Brzozowski, P. Erman, and M. Lyyra, Phys. Scr. **14**, 290 (1976).
[32] M. Mandelman, T. Carrington, and R. Young, J. Chem. Phys. **58**, 84 (1973).